Engineering 15 (2022) 186–195

Contents lists available at ScienceDirect

Engineering

journal homepage: www.elsevier.com/locate/eng

Research
Smart Grid and Energy Internet—Article

# EV Response Capability Assessment Considering User Travel Demand and Cyber System Reliability

Yanli Liu *, Ke Liu, Xu Sun

*School of Electrical and Information Engineering, Tianjin University, Tianjin 300072, China*

ARTICLE INFO

*Article history:*
Received 16 April 2021
Revised 8 August 2021
Accepted 31 August 2021
Available online 7 May 2022

*Keywords:*
Cyber system
Demand response
Electric vehicle

ABSTRACT

With the increasing penetration rate of electric vehicles (EVs), EV demand response holds great significance for promoting the optimal and secure operation of the power system. This paper proposes an EV response capability assessment method that considers EV users' travel demands and the reliability of the cyber systems integrated into both the power grid and the transportation network. A novel framework for an integrated cyber–power–transportation system is proposed for the first time, and a reliability model for the cyber system is provided. A method is further proposed to calculate the state of an EV when it is plugged in, considering the reliability of traffic guidance information and the reliability of the release of such information. The degree of relaxation in the EV charging demand is proposed to reflect the user's travel demand, based on which the EV response capability can be assessed. Extensive test results on a cyber–power–transportation system containing RBTS BUS6 and the Beijing transportation network are conducted to show the efficiency of the proposed method. The impact of cyber reliability on the EV trip and response capability is analyzed.



## 1. Introduction

Many countries have identified electric vehicles (EVs) as a national development strategy to push forward the energy transformation. EV deployment has been growing rapidly over the past 10 years, with the global stock of EVs passing 5 million in 2018. Under the new policies scenario, the global stock of EVs will exceed 130 million in 2030 [1]. With the increasing penetration rate of EVs, the charging of EVs should be dispatched well to avoid increased peak-to-valley load difference and losses, line overloads, and voltage-crossing limits in the distribution network [2]. Furthermore, as the EVs are off-road 90% of each day [3], and as EV batteries have the ability to quickly respond to system demand [4], the discharging of EVs is an important part of demand response to promote the optimal and secure operation of the power system [5]. Most of the current research on the demand response strategy of EVs [6–8] takes EV charging and discharging power as control variables, establishes relevant control models, and carries out optimization according to specific objectives, which include smoothing the renewable generation uncertainties and load fluctuation [6,9], reducing the cost or power loss [7,10,11], providing auxiliary services, and so on [2,12–15]. It is of great significance to assess the EV response capability as the fundamental link in developing a demand response strategy for EVs.

When there are a large number of EVs, the transportation network and power grid become deeply integrated in the geospatial dimension. The route choices of EV users, which are based on traffic guidance information within the transportation network, will determine the state of the EVs when they are plugged in. The EVs interact with the power grid by charging or discharging, considering their users' travel demands and the operation of the power grid. It is clear that the EV response capability strongly depends on three critical factors: ① the state of the EV when it is plugged in—namely, the state of charge (SOC) and the plug-in time; ② user travel demand, which is reflected by the expected departure time and the required SOC; and ③ the reliability of the cyber system, which directly determines the traffic guidance information and the EV response to the power grid.

At present, research on the assessment of EV response capability can be divided into two main groups. The first group takes the SOC as the index. In Refs. [16–18], the EVs discharge when the SOC exceeds the given threshold, and the EV response capability is evaluated very quickly. However, user travel demand

* Corresponding author.
*E-mail address:* yanliliu@tju.edu.cn (Y. Liu).

https://doi.org/10.1016/j.eng.2021.08.031

is ignored, and the SOC after discharging may be much less than what is required. The second group conducts an EV response capability assessment while considering user travel demand. Refs. [19,20] assume that an EV can only discharge when the SOC after discharging can meet the user's demand; however, the user's possibility for charging after discharging is ignored. Ref. [21] takes the difference between the duration of time the EV is plugged into the grid and the required charging time as the index for the discharging capability of an EV. However, it uses a relative index, which cannot reflect the absolute value of the response capability.

Three common methods are used to calculate an EV's state when it is plugged in and its travel demand—namely, the fitting method, which is based on random variables [22,23]; the trip chain method [24,25]; and the method based on spatial dimension uncertainty [26–28]. The trip chain method can make use of the users' travel destinations to build a space chain and calculate the travel time chain of the EVs in combination with the state of the transportation network to determine the travel time, mileage, and other variables of EVs. Compared with the other two methods, it can truly reflect the coupling relationship between the users' travel time and distance, while considering the impact of the transportation network on users' travel behavior. With the deep integration of the physical power network and the cyber system, the power distribution network becomes a typical cyber–physical system (CPS), which is referred to as the cyber–physical distribution network (CPDN) [29]. Furthermore, the operation and control of the smart distribution network strongly and deeply rely on the cyber system [30–34].

At present, the reliability assessment of the CPDN has been studied extensively, and this research can be divided into two main groups. The first group of research modifies the reliability model of the components in the physical power network based on an analysis of the interaction between the cyber system and the physical system; then, the consequences are analyzed and the reliability indices are calculated in a traditional way [35–37]. The second group of research focuses on specific functions that are strongly supported by the cyber system, establishes a mapping relation between cyber failure and the functions' failure, and then calculates the reliability indices [29,38,39]. Although some work on the reliability assessment of the power system has taken EVs into account, such as that in Refs. [40,41], in determining the EV response capability, the cyber systems in both the transportation network and the power grid are considered to be completely reliable, and the reliability of the cyber systems in providing reliable traffic guidance information and in the bidirectional interaction between the power grid and the EVs is ignored.

To assess the EV response capability effectively, this paper proposes a novel assessment method that considers users' travel demands and the reliability of the cyber systems integrated into both the power grid and the transportation network. First, a novel framework of an integrated cyber–power–transportation system is proposed, and a reliability model of the cyber system is provided. Next, a method is proposed to calculate the state of an EV when it is plugged in, while considering the reliability of traffic guidance information. Furthermore, the degree of relaxation in the EV charging demand is proposed to reflect user travel demand, based on which the EV response capability is assessed. Extensive test results on a cyber–power–transportation system that contains RBTS BUS6 and the Beijing transportation network are conducted to demonstrate the efficiency of the proposed method.

The rest of this paper is organized as follows. Section 2 introduces a framework of an integrated cyber–power–transportation system. A reliability model of the cyber system is presented in Section 3. Section 4 proposes a method to calculate the state of an EV when it is plugged in, considering the reliability of traffic guidance information. Section 5 further presents an EV response capability assessment method that considers EV users' travel demands. Section 6 provides case study results and a related discussion, while Section 7 summarizes and concludes this work.

## 2. Integrated cyber–power–transportation system

Fig. 1 shows the framework of the integrated cyber–power–transportation system. With the increasing number of EVs, the power grid and transportation network are integrated in the geospatial dimension. The operation and control of both the power grid and the transportation network strongly and deeply rely on cyber systems. For the power grid, the main station monitors and controls the power grid through a cyber system, and EV aggregators are adopted between the main station and the EVs to exchange information and manage the charging and discharging of the EVs. For the transportation network, the traffic control center collects real-time traffic data, and then generates and releases traffic guidance information, based on which travel route selections for the EVs are generated. The basic structure of the cyber systems in the power grid and transportation network are described below.

### 2.1. Cyber system of the power grid

The cyber system of the power distribution network consists of a backbone layer and an access layer, as shown in Fig. 2. The backbone layer is the network between the main station and the substations and EV aggregators, based on the synchronous digital hierarchy (SDH). The access layer includes two parts: the network between the substations and the intelligent electronic devices (IEDs), which is based on an ethernet passive optical network (EPON) that includes optical line terminals (OLTs) and optical network units (ONUs); and the network between the EV aggregators and the EVs, which is based on EPON and Wi-Fi.

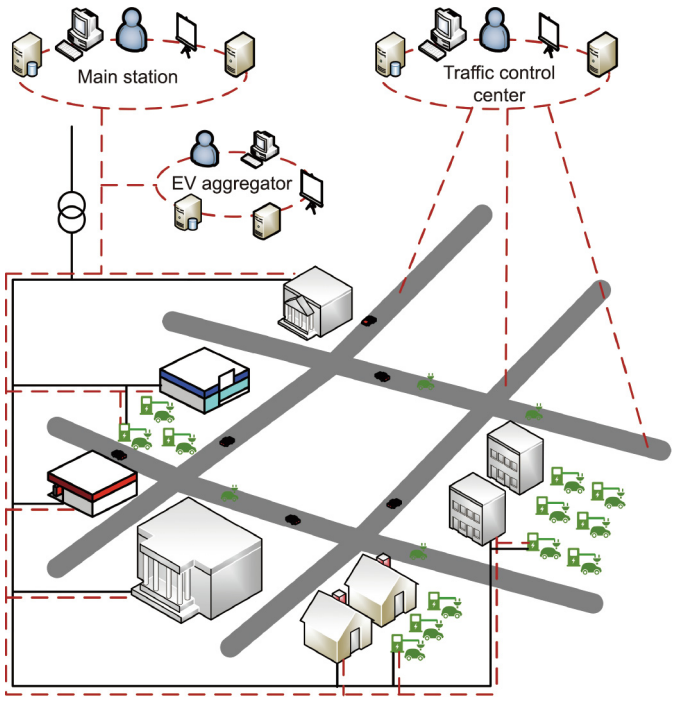


**Fig. 1.** Framework of the integrated cyber–power–transportation system.

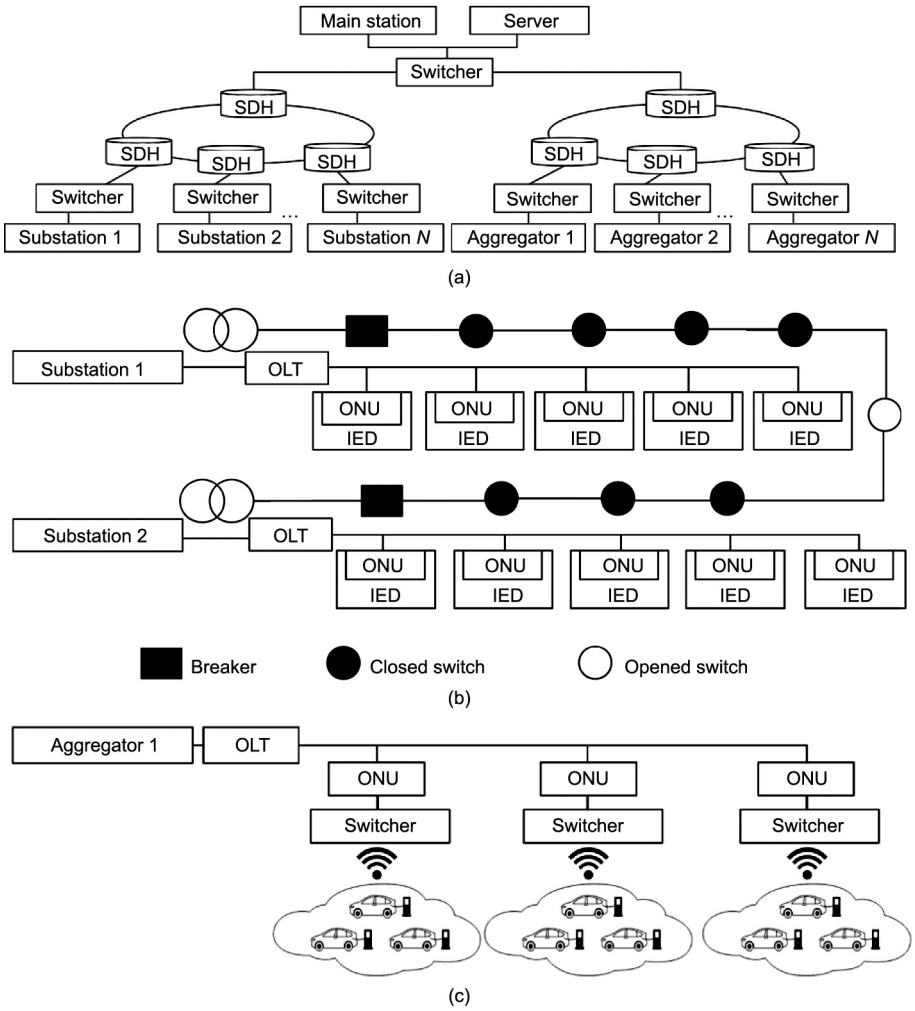


**Fig. 2.** The cyber system of the power distribution network. (a) Backbone layer between the main station and substations and aggregators; (b) access layer between substations and IEDs; (c) access layer between EV aggregators and EVs.

### *2.2. Cyber system of the transportation network*

The cyber system of the transportation network consists of a traffic control center, traffic substations, traffic information-collecting devices, and so forth. Fig. 3 shows the basic structure, in which the backbone layer adopts SDHs to connect the traffic control center and traffic substations, while the access layer adopts EPON to connect the traffic substations and the detectors. The traffic control center collects traffic data, generates and releases traffic guidance information, and dispatches the transportation network. As the most widely used traffic information-collecting device, ring induction coil detectors are selected here.

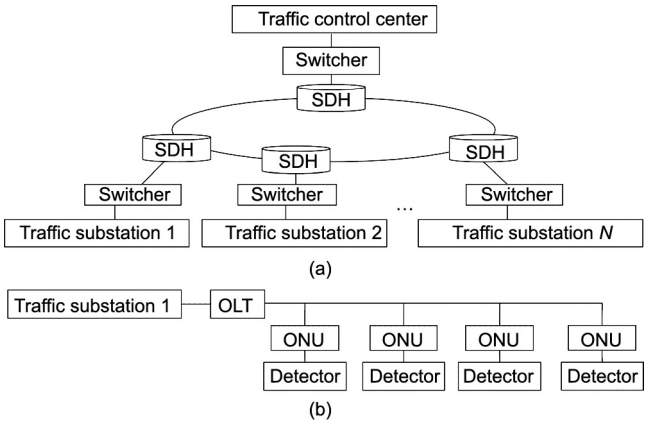


**Fig. 3.** Basic structure of the cyber system of the transportation network. (a) Backbone layer; (b) access layer.

Meanwhile, the traffic control center itself is a LAN-based system [42], including database servers, application servers, dispatchers, and so forth. The database server stores traffic data and traffic guidance information; then, the application server extracts information and transmits it to different release platforms. Fig. 4 shows the basic cyber structure of the traffic guidance information release, in which two database servers and two application servers are adopted to improve the reliability.

Consequently, the reliability of the cyber system in both Figs. 3 and 4 will affect the traffic guidance information and the release of traffic guidance information, respectively.

## 3. Reliability model of the cyber system

### *3.1. Reliability of physical components*

A two-state Markov model is used to describe the failure and repair of physical components. Operating state duration (the time

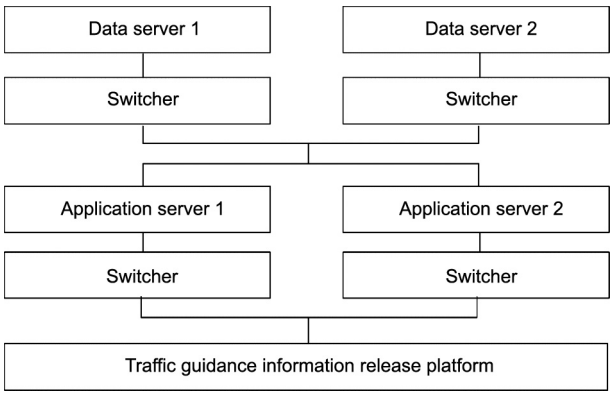


**Fig. 4.** Basic cyber structure of the traffic guidance information release.

to failure, TTF) and outage state duration (the time to repair, TTR) can be further calculated as shown in Eqs. (1) and (2):

$$\mathrm{TTF} = -(1/\lambda)\ln u_1 \tag{1}$$

$$\mathrm{TTR} = -(1/\mu)\ln u_2 \tag{2}$$

where $\lambda$ and $\mu$ are the failure rate and repair rate, and $u_1$ and $u_2$ are random numbers that are subject to the uniform distribution in [0, 1].

### 3.2. Reliability of information transmission

Information, such as measurement data and control signals, is transmitted through the communication network. The connectivity and performance of the communication network determine the reliability of the information transmission.

#### 3.2.1. Connectivity of the communication network

The communication network can be represented by an undirected connected graph, set as $\boldsymbol{G} = (V, E)$. All components are regarded as nodes (including the communication lines), which are represented by $V = \{v_1, v_2, \ldots, v_n\}$, and the connection relationships between nodes are regarded as edges, which are denoted by $E = \{e_1, e_2, \ldots, e_n\}$. An adjacency matrix $\boldsymbol{A}(\boldsymbol{G}) = a_{xy(n\times n)}$ can be defined as follows:

$$a_{xy} = \begin{cases} 1, & v_x \text{ is directly connected to } v_y, \text{ and } x \neq y \\ 0, & \text{else} \end{cases} \tag{3}$$

where $\boldsymbol{G}$ is an undirected connected graph representing the communication network; $V$ is the set of nodes $v$; $E$ is the set of edges $e$; $x$ and $y$ are the numbers of the corresponding nodes.

The reachability matrix $\boldsymbol{P} = p_{xy(n\times n)}$ is used to describe the connection relationship $p_{xy}$ between nodes $v_x$ and $v_y$, which can be defined as follows:

$$p_{xy} = \begin{cases} 1, & v_x \text{ is connected to } v_y \\ 0, & v_x \text{ is not connected to } v_y \end{cases} \tag{4}$$

The $k$-step reachability matrix is calculated as follows:

$$\boldsymbol{M} = \boldsymbol{I} + \boldsymbol{A} + \boldsymbol{A}^2 + \cdots + \boldsymbol{A}^k \tag{5}$$

Then the non-zero element in $\boldsymbol{M}$ is set to 1 to obtain the reachability matrix $\boldsymbol{P}$, and the network connectivity can be determined.

#### 3.2.2. Performance of the communication network

The performance of the communication network can be evaluated in terms of information delay, packet loss, bit error, and so on. After the end-to-end information transmission is completed, the receiving end will return a response packet to confirm whether the information has been reliably transmitted. Data retransmission can effectively avoid the impact of packet loss and bit error. Therefore, the transmission delay is considered and the uncertainties of the transmission delay are modeled as a normal distribution [43]. The transmission will be unsuccessful if the delay exceeds the given threshold.

## 4. State of plugged-in EV considering the reliability of traffic guidance information

### 4.1. Route selection considering the reliability of traffic guidance information

Since travel time is the most important factor for users to select routes, it is assumed that users select the route with the shortest travel time, according to Eqs. (6)–(8):

$$\min \sum c_{rs}(t) \tag{6}$$

$$c_{rs}(t) = l_{rs}/v_{rs}(t) = l_{rs}\cdot[1 + (V_{rs}(t)/C_{rs})^{\beta}]/(\alpha_1 \cdot v_{rs,0}) \tag{7}$$

$$\begin{cases} v_{rs}(t) = \alpha_1 \cdot v_{rs,0}/[1 + (V_{rs}(t)/C_{rs})^{\beta}] \\ \beta = \alpha_2 + \alpha_3 \cdot (V_{rs}(t)/C_{rs})^3 \end{cases} \tag{8}$$

where $r$, $s$ are the nodes at the two ends of the road respectively; $c_{rs}(t)$ is the time impedance—namely, the required time to pass road $(r, s)$; $V_{rs}(t)$ is the traffic flow collected by the ring induction coil detectors; $l_{rs}$ and $v_{rs}(t)$ are the length and traffic speed of road $(r, s)$; $v_{rs,0}$ and $C_{rs}$ are the designed traffic speed and traffic capacity of road $(r, s)$, respectively; and $\alpha_1$, $\alpha_2$, and $\alpha_3$ are the given model parameters.

Considering the reliability of the cyber system in Fig. 3, failure of cyber components and information transmission may result in detector data loss, and the average values of the data in adjacent time periods will be used to fill in for the missing data [44]. $V_{rs}(t)$ and $c_{rs}(t)$ will be updated as follows:

$$V_{rs}^1(t) = \frac{1}{n}[V_{rs}(t-n) + V_{rs}(t-n-1) + \cdots + V_{rs}(t-1)] \tag{9}$$

$$c_{rs}^1(t) = l_{rs}[1 + (V_{rs}^1(t)/C_{rs})^{\beta}]/(\alpha_1 \cdot v_{rs,0}) \tag{10}$$

Considering the reliability of the cyber system in Fig. 4, the release of traffic guidance information may fail, and EV users will select travel routes based on their perceived impedance $c_{rs}^2(t)$, which is shown as follows:

$$c_{rs}^2(t) = c_{rs}(t) + \Delta c_{rs}(t) \tag{11}$$

where $\Delta c_{rs}(t)$ is the deviation of the time impedance, which follows the Gumbel distribution with a mean value of 0.

In summary, the routes will be selected based on Eqs. (12) and (13), considering the reliability of the traffic guidance information.

$$\min \sum c'_{rs}(t) \tag{12}$$

$$c'_{rs}(t) = \begin{cases} c_{rs}(t), & \text{completely reliable} \\ c_{rs}^1(t), & \text{unreliable generation} \\ c_{rs}^2(t), & \text{unreliable release} \end{cases} \tag{13}$$

### 4.2. State of EV when plugged in

A trip chain is used to simulate an EV user's daily traveling. As shown in Fig. 5, the trip chain of user $i$ consists of a space chain and a time chain:

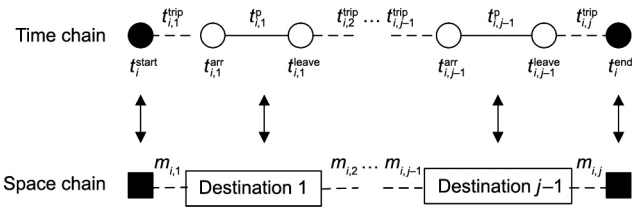


**Fig. 5.** The trip chain.

(1) **Space chain:** The node represents the user's travel destination, the line between two nodes represents the user's driving path, and the mileage of the $j$th trip is $m_{i,j}$.

(2) **Time chain:** The node represents the time node, $t_i^{\text{start}}$ and $t_i^{\text{end}}$ represent the starting time and ending time of the daily trip, respectively, and $t_{i,j}^{\text{arr}}$ and $t_{i,j}^{\text{leave}}$ represent the arriving time and leaving time at the $j$th destination, respectively. The dashed line and the corresponding $t_{i,j}^{\text{trip}}$ represent the travel time between two destinations. The solid line and the corresponding $t_{i,j}^{\text{p}}$ represent the stay time at destination $j$.

The method of calculating variables in the trip chain is introduced further below.

*4.2.1. Space chain*

(1) **EV daily travel schedule.** An activity sampling-based travel schedule model [45] is used to generate the space chain. The residential area is the starting and ending area of the daily travel, and destinations include the working area, shopping mall, hospital, residential area (i.e., returning home partway through the day), and scenic spot. The EV daily travel schedule can be sampled based on the statistical probabilities of the variable activities. If the destinations include the working area, then the working area should be placed in the first position. If the destinations include the residential area (i.e., returning home partway through the day), then it should be placed in a random position, excluding the beginning and end of all destinations. Other destinations are randomly scheduled.

(2) **Mileage $m_{i,j}$ considering the reliability of traffic guidance information.** As introduced in Section 4.1, users select a route according to Eqs. (12) and (13), and then $m_{i,j}$ and the related power consumption $\Delta\text{SOC}_{i,j}$ can be calculated as follows:

$$m_{i,j} = \sum_{(r,s)\in S} l_{rs} \tag{14}$$

$$\Delta\text{SOC}_{i,j} = \sum_{(r,s)\in S} w_{rs}(t)\cdot l_{rs}/B \tag{15}$$

where $S$ is the set of all roads of the selected route; $w_{rs}(t)$ is the power consumption of the EV for 1 km, calculated by the method provided in Ref. [46]; and $B$ is the capacity of the EV battery.

*4.2.2. Time chain*

(1) **The starting time of the daily trip.** The $t_i^{\text{start}}$ follows a normal distribution [47]:

$$f_{t_i^{\text{start}}}(t) = \frac{1}{\sigma_1\sqrt{2\pi}} e^{-(t-\mu_1)^2/(2\sigma_1^2)} \tag{16}$$

where $\mu_1$ = 7.8 and $\sigma_1$ = 1.5.

(2) **The travel time between two destinations.** The $t_{i,j}^{\text{trip}}$ can be calculated as follows:

$$t_{i,j}^{\text{trip}} = \sum_{(r,s)\in S} c'_{rs}(t) \tag{17}$$

(3) **The leaving time at the $j$th destination.** If the trip starts from the working area, then $t_{i,j}^{\text{leave}}$ is the departure time from the working area, $t_i^{\text{wdep}}$, which follows a normal distribution [47]:

$$f_{t_i^{\text{wdep}}}(t) = \frac{1}{\sigma_2\sqrt{2\pi}} e^{-(t-\mu_2)^2/(2\sigma_2^2)} \tag{18}$$

where $\mu_2$ = 17.5 and $\sigma_2$ = 0.5.

If the trip starts in other areas, then $t_{i,j}^{\text{leave}}$ can be calculated as follows:

$$t_{i,j}^{\text{leave}} = t_{i,j}^{\text{arr}} + t_{i,j}^{\text{stay}} \tag{19}$$

$$f_{t_{i,j}^{\text{stay}}}(t) = \frac{1}{\sigma_3\sqrt{2\pi}} e^{-(t-\mu_3)^2/(2\sigma_3^2)} \tag{20}$$

where $t_{i,j}^{\text{stay}}$ is the stay time at a non-work destination $j$, $\mu_3$ = 1.5, and $\sigma_3$ = 0.5.

*4.2.3. Fast charging analysis*

Users will change their route and select the nearest EV charging station for fast charging if the SOC meets the following condition:

$$\text{SOC}_i^{t_{i,j}^{\text{leave}}} - \Delta\text{SOC}_{i,j+1} < 0.2 \tag{21}$$

Existing fast chargers at EV charging stations generally charge the SOC to about 80% at high power, and then slowly charge it at low power. Therefore, the user is considered to leave the charging station after the SOC reaches 80%. The time for fast charging can be calculated as follows:

$$t_{i,\text{charge}} = [0.8 - (\text{SOC}_i^{t_{i,j}^{\text{leave}}} - \Delta\text{SOC}_{i,\text{station}})]B_i/P_{\text{chf}} \tag{22}$$

where $\Delta\text{SOC}_{i,\text{station}}$ is the power consumption from the current destination to the charging station, and $P_{\text{chf}}$ is the rated fast charging power.

*4.3. Procedure for calculating the state of an EV when plugged in*

Fig. 6 outlines the procedure for calculating the state of an EV when it is plugged in.

## 5. EV response capability assessment considering user demand

*5.1. EV charging strategy*

EVs spend most of the time parked in residential and working areas, with a relatively short time spent in other areas. In the main distribution station–aggregator hierarchical control structure, when EV $i$ is plugged into the grid in a residential or working area, the following charging optimization will be performed by the aggregator to minimize the total load variance of the system.

$$\min \sum_{t=1}^{T} \left(P_{\text{ch},i}(t) + P_{i-1}(t) - \bar{P}\right)^2 \tag{23}$$

s.t.

$$\text{SOC}_i^{t_{\text{leave}}} \geq \text{SOC}_i^{\text{d}} \tag{24}$$

$$0.2 \leq \text{SOC}_i(t) \leq 1 \tag{25}$$

$$(1 - D_{\text{Plug},i}(t))\cdot P_{\text{ch},i}(t) = 0 \tag{26}$$

$$P_{\text{ch},i}(t) = \{0,\ P_{\text{chr},i}\} \tag{27}$$

where $P_{\text{ch},i}(t)$ is the charging power of the $i$th EV at time $t$; $P_{i-1}(t)$ is the total load, including the previous 1 to $i-1$ EVs at time $t$; $\bar{P}$ is the

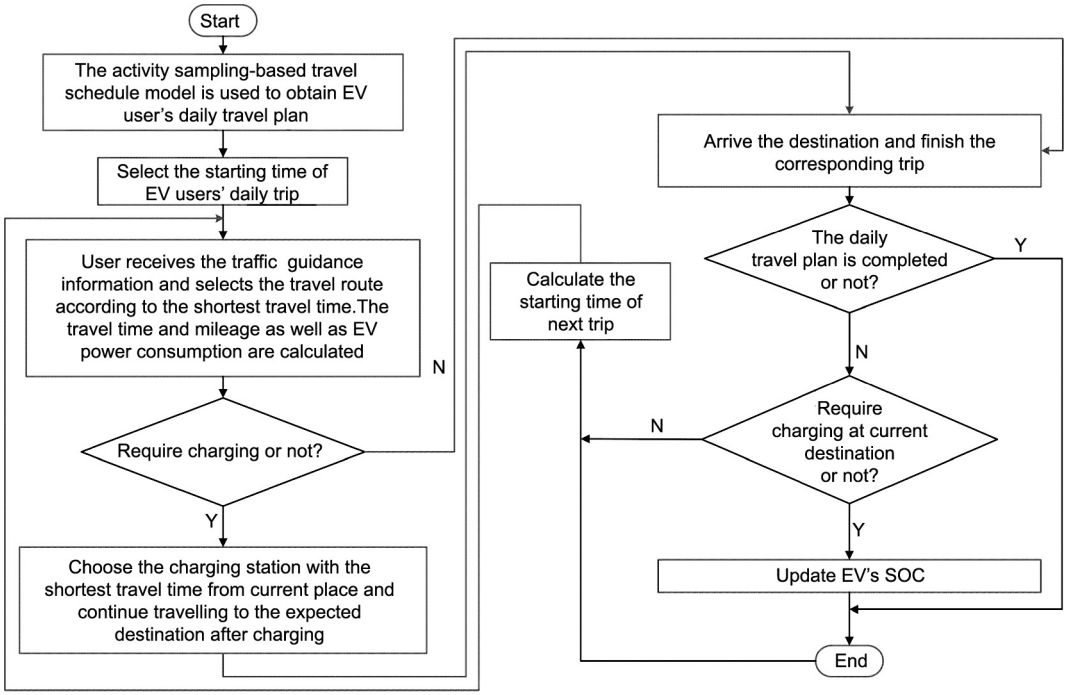


**Fig. 6.** Procedure for calculating the state of an EV when it is plugged in.

average load within the optimization period $T$; $SOC_i^d$ is the SOC demand; and $P_{chr,i}$ is the rated charging power. $D_{Plug,i}(t) = 1$ if the EV is plugged in; otherwise, $D_{Plug,i}(t) = 0$.

The variables in Eqs. (23)–(27) can be calculated as follows:

$$SOC_i^{t_{leave}} = SOC_i^{t_{arrive}} + \sum_{t=t_{arrive}}^{t_{leave}} P_{ch,i}(t)/B_i \tag{28}$$

$$D_{Plug,i}(t) = \begin{cases} 1, & t_{arr,i} < t < t_{leave,i} \\ 0, & \text{others} \end{cases} \tag{29}$$

$$\bar{P} = \sum_{t=1}^{T} \left( \sum P_{ch,i}(t) + P(t) \right) / T \tag{30}$$

$$P_{i-1}(t) = P_0(t) + \sum_{j=1}^{i-1} P_{ch,j}(t) \cdot s_{j,j+1} \tag{31}$$

$$SOC_i^{t_{arrive}} = 1 - \sum w_{rs} \cdot l_{rs}/B_i + \sum SOC_i^{ch} \tag{32}$$

where $SOC_i^{ch}$ represents the fast charging power at the charging station; $s_{j,j+1}$ represents the state of communication between the aggregator with the $(j + 1)$th EV and the aggregator with the $j$th EV; $s_{j,j+1} = 1$ means that the communication is successful; and $s_{j,j+1} = 0$ means that the communication is unsuccessful.

### 5.2. EV response capability based on the degree of relaxation in the EV charging demand

The degree of relaxation in the EV charging demand is proposed as follows:

$$L_i(t) = t_{leave,i} - t - (SOC_i^d - SOC_i(t))B_i/P_{chr,i} \tag{33}$$

where $t_{leave,i} - t$ represents the remaining rechargeable time of the $i$th EV at moment $t$; and $(SOC_i^d - SOC_i(t))B_i/P_{chr,i}$ represents the remaining required charging time to meet the $i$th EV travel demand at moment $t$. Therefore, $L_i(t)$ represents the urgency of the $i$th EV charging at moment $t$, where the smaller $L_i(t)$ is, the stronger the EV charging demand is and the weaker the response capability is.

According to $L_i(t)$, EVs can be classified as follows:

(1) $L_i(t) < 0$: User demand cannot be satisfied even if EV is continuous charged.

(2) $0 \le L_i(t) < \Delta t$: If EV is charged continuously from now until the departure time; user demand can be satisfied, but the charging process must be uninterrupted.

(3) $\Delta t \le L_i(t) < \Delta t(1 + P_{dis,i}/P_{chr,i})$: The EV charging process can be interrupted, but if the EV discharges, user demand cannot be satisfied.

(4) $L_i(t) \ge \Delta t(1 + P_{dis,i}/P_{chr,i})$: The charging process can be interrupted and the EV can discharge, where $\Delta t$ is the unit time for optimal scheduling and $P_{dis,i}$ is the rated discharging power.

To reduce damage to the EV battery, the EV SOC should not be less than 20%, and the EV that can discharge at time $t$ should satisfy Eq. (34):

$$\begin{cases} L_i(t) \ge \Delta t(1 + P_{dis,i}/P_{chr,i}) \\ D_{Plug,i}(t) = 1 \\ SOC_i(t) - P_{dis,i}/B_i \ge 0.2 \end{cases} \tag{34}$$

Then, the EV response capability $P_i^{rc}(t)$ considering the user demand at time $t$ is

$$P_i^{rc}(t) = \begin{cases} P_{dis,i}, & \text{Eq. (34) is satisfied} \\ 0, & \text{others} \end{cases} \tag{35}$$

To describe the relationship between the EV SOC when the user leaves and the user's travel demand, EV user satisfaction is defined as follows:

$$R = N_s/N \tag{36}$$

where $N$ is the total number of EVs, and $N_s$ is the number of EVs with enough SOC that can meet the user travel demand after leaving.

## 6. Case study

As shown in Fig. 7, a system containing RBTS BUS6 [48] (upper layer) and the Beijing transportation network (lower layer) was taken as a study case. The transportation network formed by the expressway (red line) and the main road (blue line) within the fifth ring road in Beijing is equivalent to a 25 km × 25 km connected graph, in which the road network node is placed on a corresponding grid node with a unit length of 1 km. There are 2370 EVs, given that the penetration rate of EVs is 50% and the ratio of private vehicles to residential users is 1.86 [47]. The load points in RBTS BUS6 corresponding to the Beijing transportation network are given in Table 1. The reliability parameters of cyber components and detailed information on RUTS BUS6 and the Beijing transportation network can be found in Refs. [48–51]. The simulations were realized through the MATLAB platform, with a focus on day-ahead optimization scenarios with 1 h increments.

### 6.1. Assessment of EV response capability

Case 1: EVs can discharge if the proposed Eq. (34) is satisfied.

Case 2: EVs can discharge if the SOC is higher than a certain threshold, which is set at 80%, 70%, 60%, and 50%, respectively [16].

Case 3: EVs can discharge only when the SOC after discharging is higher than the users' demand [20].

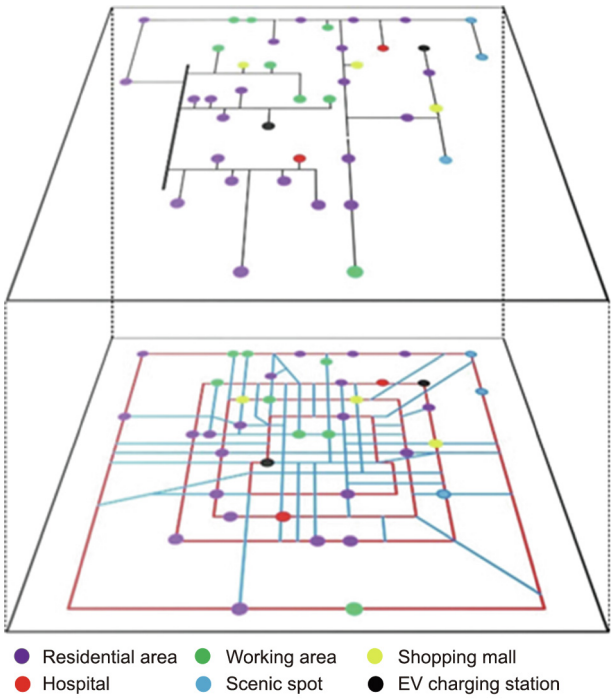


**Fig. 7.** Power distribution network–transportation system of the study case.

**Table 1**
Load points in RBTS BUS6 corresponding to the Beijing transportation network.

| Area | Load points |
|---|---|
| Residential area | 1, 2, 3, 4, 7, 8, 9, 10, 11, 13, 18, 19, 22, 23, 25, 27, 28, 29, 31, 33, 36, 39 |
| Working area | 6, 14, 16, 17, 20, 21, 24, 30 |
| Shopping mall | 15, 26, 38 |
| Hospital | 12, 32 |
| Scenic spot | 34, 35, 37 |
| Charging station | 5, 40 |

The EV response capability for different cases in the residential area is given in Fig. 8. Apparent differences can be found between the cases. The response capability in Case 3 is significantly lower than that in the other two cases, because the SOC of most of the EVs that just came back cannot meet the users' subsequent travel demands. Case 1 has a higher response capability than Case 2 from 11:00 on one day to 2:00 the next day, using a 24 h clock. After 2:00, the response capability of Case 1 decreases and is lower than that of Case 2, because the users' demands should always be met in Case 1, and discharging may prevent the users' demands from being met due to the approaching departure time.

Fig. 9 depicts EV users' satisfaction in the residential area. User satisfaction in Case 1 and Case 3 is always 1. In Case 2, user satisfaction remains close to 1 from 12:00 to 24:00, but decreases significantly from 1:00 to 11:00; furthermore, the lower the SOC threshold is, the lower the satisfaction is.

As shown in Figs. 10 and 11, the EV response capability and EV user satisfaction in different cases in the working area are similar to those in the residential area. It is worth noting that the response capability in Case 2 is almost the same with thresholds of 50% and 60%. This is because the number of EVs with a SOC of 50%–60% in the working area is almost 0, as shown in Fig. 12.

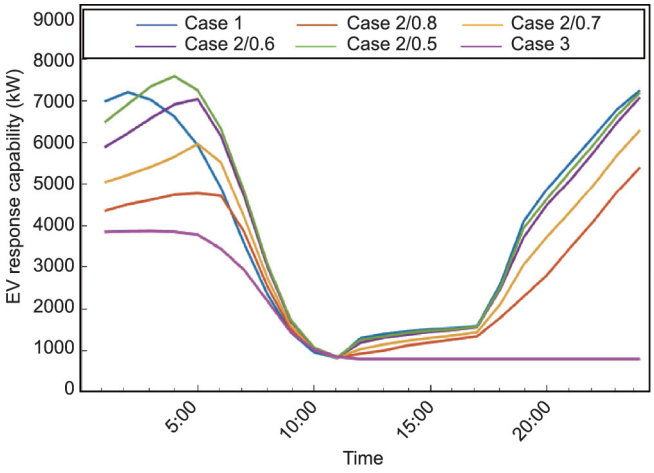


**Fig. 8.** EV response capability in the residential area.

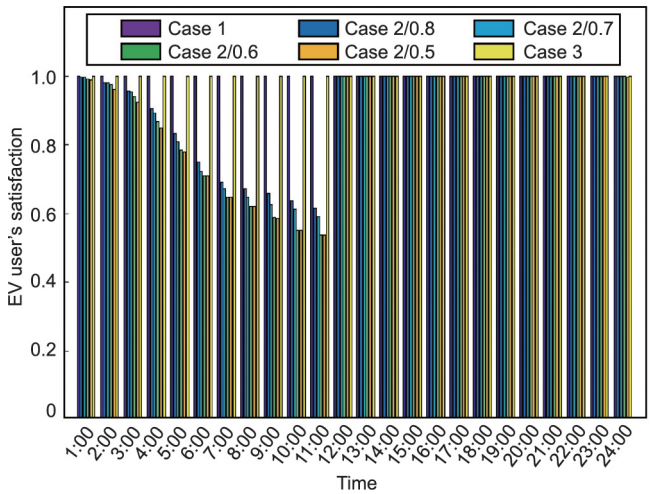


**Fig. 9.** EV user's satisfaction in the residential area.

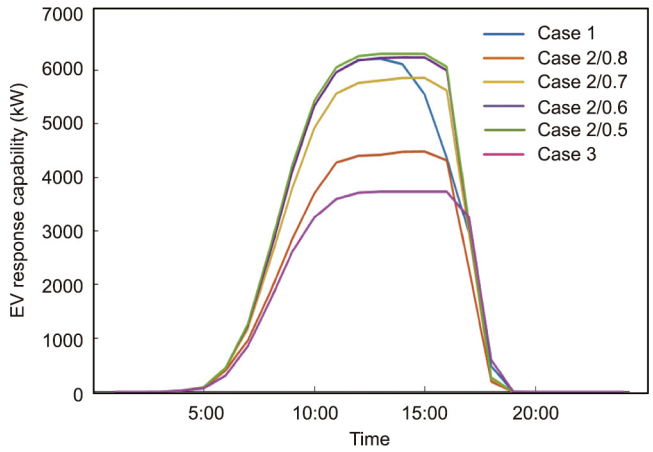


**Fig. 10.** EV response capability in the working area.

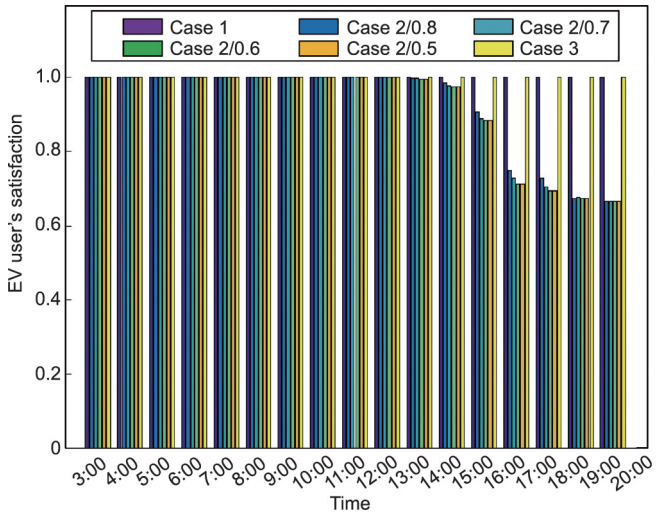


**Fig. 11.** EV user's satisfaction in the working area.

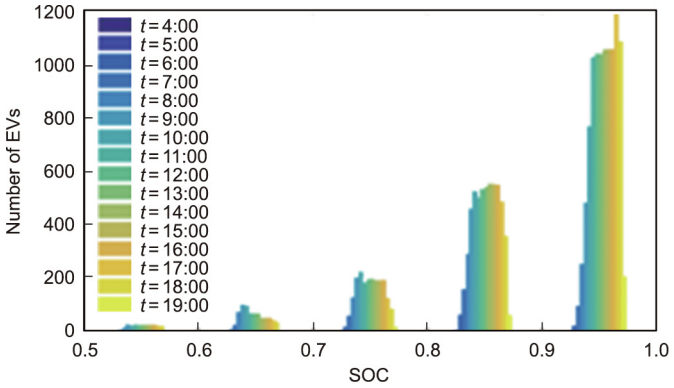


**Fig. 12.** EV SOC distribution in the working area.

It can be seen that the EV response capability can be maximized to meet the users' travel demand by means of the proposed method.

### 6.2. Impact of traffic guidance information on EV trips

Table 2 provides the simulation result for EV trips, considering the reliability of traffic guidance information (i.e., its generation) and the reliability of its release. When the traffic guidance information is completely reliable, EV users can accurately identify the traffic network state and choose the routes that take the shortest time. However, mileage and power consumption may increase. In contrast, unreliable traffic guidance information or the unreliable release of information will cause an obvious increase in the average daily travel time, as well as delays in arriving at the working area and returning to the residential area. Figs. 13 and 14 provide the probability distribution of the EVs' arrival time at the working area and return time at the residential area. It can be found that the probability distributions of time corresponding to unreliable traffic guidance information and the unreliable release of such information are relatively close and significantly lag behind the probability distribution with completely reliable traffic guidance information.

**Table 2**
Impact of traffic guidance information on EV trips.

| EV trip data | Completely reliable | Unreliable generation | Unreliable release |
|---|---|---|---|
| Average daily travel time (h) | 1.7101 | 2.8367 | 2.6082 |
| Average daily mileage (km) | 46.4090 | 46.1728 | 42.4838 |
| Average time of arriving at the working area | 8.3527 | 8.6306 | 8.6051 |
| Average time of returning to the residential area | 19.1347 | 19.9713 | 19.7362 |
| Average daily power consumption | 0.5158 | 0.5174 | 0.4817 |
| Proportion of fast charging | 10.9243% | 11.2978% | 7.1428% |
| Average fast charging energy | 0.0713 | 0.0723 | 0.0463 |

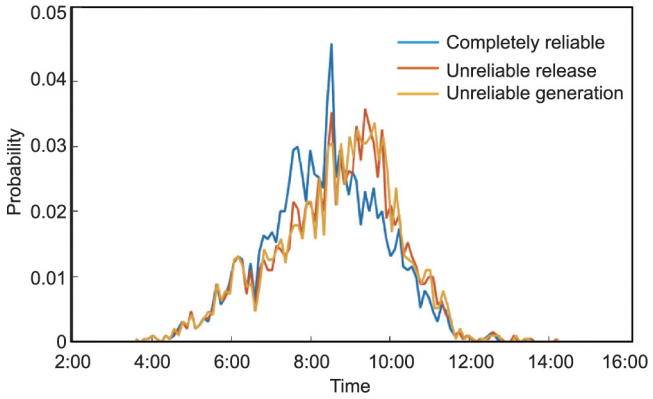


**Fig. 13.** Probability distribution of EVs' arrival time at the working area.

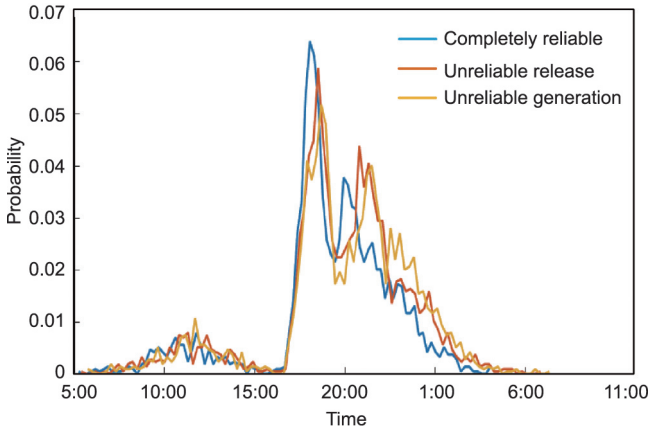


**Fig. 14.** Probability distribution of EVs' return time at the residential area.

With the unreliable release of traffic guidance information, users who select routes based on their own perceived impedance within the traffic network may select routes with the shortest mileage instead of the shortest time, so the users' travel time becomes longer, while the parameters related to the driving mileage, such as the average daily mileage, average daily power consumption, proportion of fast charging, and average fast charging energy, become smaller.

### 6.3. Impact of the reliability of cyber systems on EV response capability

Case 1: The cyber systems are completely reliable.

Case 2: The cyber system of the power distribution network is completely reliable, and the reliability of the transportation cyber system is considered.

Case 3: The transportation cyber system is completely reliable, and the reliability of the cyber system of the power distribution network is considered.

Case 4: The reliability of the cyber systems of both the transportation network and the power distribution network are considered.

Fig. 15 shows the EV response capability of different cases at the working area and residential area. It is clear that the reliability of the cyber system has a great impact on the EV response capability, which is lower in Cases 2–4 than in Case 1. The reliability of the transportation cyber system mainly affects the EV response capability during the centralized plug-in time of the EVs, while the reliability of the cyber system of the power distribution network affects the EV response capability all the time and to a greater extent. This is because multiple real-time communications and links are required in the control of EV charging/discharging, which raises the probability of unreliable information transmission, and results in part of the EVs being in an uncontrollable state and a significant decrease in the system response capability.

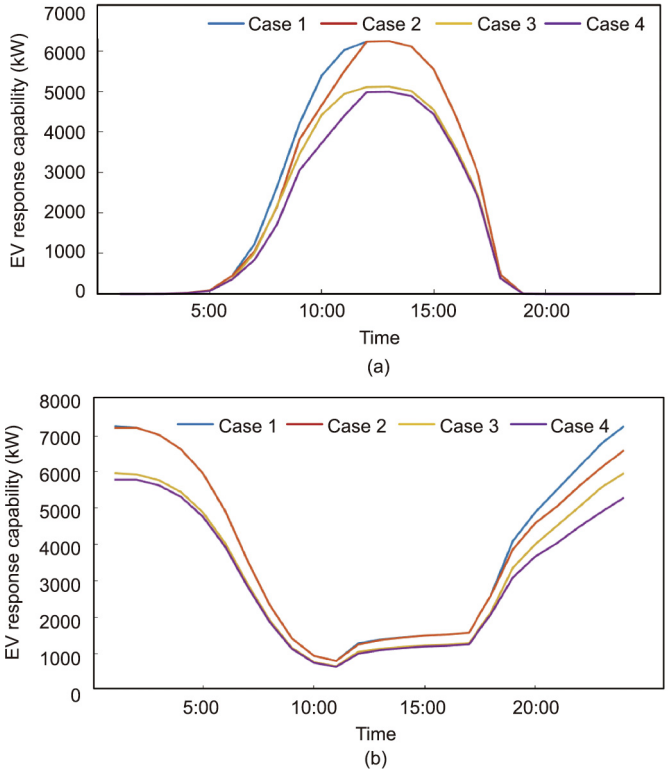


**Fig. 15.** EV response capability of different cases at (a) the working area and (b) the residential area.

## 7. Conclusions

This paper proposes an EV response capability assessment method that considers EV users' travel demand and the reliability of the cyber systems integrated into both the power grid and the transportation network. The simulation results of the improved system, which includes the Beijing transportation network and RBTS BUS6, show that the proposed method, based on the degree of relaxation in the EV charging demand, can maximize the EV response capability while always satisfying the users' travel demand. Unreliable traffic guidance information or the unreliable release of such information will affect EV trips and eventually delay the EV plug-in time. The reliability of the cyber system has a great impact on the EV response capability, with the cyber system of the power distribution network having a greater impact than that of the transportation cyber system.

The proposed method not only assesses the EV response capability more accurately and effectively than other current methods, but also supports the joint planning and optimal operation of cyber–power–transportation systems. Furthermore, the impacts of the transportation cyber system are only considered from the aspect of traffic guidance information in this paper. The function of the transportation cyber system on transportation system dispatching will be considered in our future work. In addition, the dynamic thermal rating (DTR) system holds strong potential for upgrading the power grid. Given the many sensors and aggregators in the DTR, extensive communication among them cannot be ignored. Therefore, in order to deal with the line-overloading problem that may be caused by plug-in EVs, the reliability of the DTR cyber system will be considered in our future work. Given the increasing risk of cyberattacks, which may lead to transmission interruptions, transmission delays, information tampering, and other failures in cyber systems, the effects of cyberattacks on EV response capability in CPDN cannot be ignored. The first two effects have been discussed in this paper; information tampering will also be studied in the future.

## Acknowledgments

This work was supported by the National Key Research and Development Program of China (2017YFB0903000), and the Basic Theories and Methods of Analysis and Control of the Cyber Physical System for Power Grid.

## Compliance with ethics guidelines

Yanli Liu, Ke Liu, and Xu Sun declare that they have no conflict of interest or financial conflicts to disclose.

## References

[1] International Energy Agency. Global EV outlook 2019 [Internet]. Paris: International Energy Agency; 2019 May [cited 2021 Apr 15]. Available from: https://www.iea.org/reports/global-ev-outlook-2019.
[2] Godina R, Rodrigues EMG, Matias JCO, Catalão JPS. Smart electric vehicle charging scheduler for overloading prevention of an industry client power distribution transformer. Appl Energy 2016;178:29–42.
[3] Willett K, Steven EL. Electric vehicles as a new power source for electric utilities. Transp Res D Transp Environ 1997;2(3):157–75.
[4] Han S, Han S, Sezaki K. Development of an optimal vehicle-to-grid aggregator for frequency regulation. IEEE Trans Smart Grid 2010;1(1):65–72.
[5] Zhong W, Xie K, Liu Y, Yang C, Xie S. Topology-aware vehicle-to-grid energy trading for active distribution systems. IEEE Trans Smart Grid 2019;10(2):2137–47.
[6] Li Y, Hu B. A consortium blockchain-enabled secure and privacy-preserving optimized charging and discharging trading scheme for electric vehicles. IEEE Trans Industr Inform 2021;17(3):1968–77.
[7] Singh J, Tiwari R. Cost benefit analysis for V2G implementation of electric vehicles in distribution system. IEEE Trans Ind Appl 2020;56(5):5963–73.

[8] Lu X, Chan KW, Xia S, Shahidehpour M, Ng WH. An operation model for distribution companies using the flexibility of electric vehicle aggregators. IEEE Trans Smart Grid 2021;12(2):1507–18.
[9] Zhang X, Chan KW, Wang H, Zhou B, Wang G, Qiu J. Multiple group search optimization based on decomposition for multi-objective dispatch with electric vehicle and wind power uncertainties. Appl Energy 2020;262:114507.
[10] Zhang H, Hu Z, Xu Z, Song Y. Evaluation of achievable vehicle-to-grid capacity using aggregate PEV model. IEEE Trans Power Syst 2017;32(1):784–94.
[11] Mehta R, Verma P, Srinivasan D, Yang J. Double-layered intelligent energy management for optimal integration of plug-in electric vehicles into distribution systems. Appl Energy 2019;233:146–55.
[12] Zhao J, Wan C, Xu Z, Wong KP. Spinning reserve requirement optimization considering integration of plug-in electric vehicles. IEEE Trans Smart Grid 2017;8(4):2009–21.
[13] Pavić I, Capuder T, Kuzle I. Value of flexible electric vehicles in providing spinning reserve services. Appl Energy 2015;157:60–74.
[14] Wang Q, Zhang C, Ding Y, Xydis G, Wang J, Østergaard J. Review of real-time electricity markets for integrating distributed energy resources and demand response. Appl Energy 2015;138:695–706.
[15] Sharma A, Srinivasan D, Trivedi A. A decentralized multi-agent approach for service restoration in uncertain environment. IEEE Trans Smart Grid 2018;9(4):3394–405.
[16] Hou K, Xu X, Jia H, Yu X, Jiang T, Zhang K, et al. A reliability assessment approach for integrated transportation and electrical power systems incorporating electric vehicles. IEEE Trans Smart Grid 2018;9(1):88–100.
[17] Sharma A, Srinivasan D, Trivedi A. A decentralized multiagent system approach for service restoration using DG islanding. IEEE Trans Smart Grid 2015;6(6):2784–93.
[18] Ma Y, Houghton T, Cruden A, Infield D. Modeling the benefits of vehicle-to-grid technology to a power system. IEEE Trans Power Syst 2012;27(2):1012–20.
[19] Das R, Wang Y, Putrus G, Kotter R, Marzband M, Herteleer B, et al. Multi-objective techno-economic-environmental optimisation of electric vehicle for energy services. Appl Energy 2020;257:113965.
[20] Li Z, Zhao S, Liu Y. Control strategy and application of distributed electric vehicle energy storage. Power Syst Technol 2016;40(2):442–50. Chinese.
[21] Yang X, Ren S, Zhang Y, Zhao B, Huang F, Xie L. Schedulable ability model and priority-based intraday scheduling strategy for electric vehicle. Autom Electr Power Syst 2017;41(2):84–93. Chinese.
[22] Rautiainen A, Repo S, Jarventausta P, Mutanen A, Vuorilehto K, Jalkanen K. Statistical charging load modeling of PHEVs in electricity distribution networks using national travel survey data. IEEE Trans Smart Grid 2012;3(4):1650–9.
[23] Arias MB, Kim M, Bae S. Prediction of electric vehicle charging-power demand in realistic urban traffic networks. Appl Energy 2017;195:738–53.
[24] Tao S, Liao K, Xiao X, Wen J, Yang Y, Zhang J. Charging demand for electric vehicle based on stochastic analysis of trip chain. IET Gener Transm Distrib 2016;10(11):2689–98.
[25] Tang D, Wang P. Probabilistic modeling of nodal charging demand based on spatial-temporal dynamics of moving electric vehicles. IEEE Trans Smart Grid 2016;7(2):627–36.
[26] Steen D, Tuan LA, Carlson O, Bertling L. Assessment of electric vehicle charging scenarios based on demographical data. IEEE Trans Smart Grid 2012;3(3):1457–68.
[27] Bae S, Kwasinski A. Spatial and temporal model of electric vehicle charging demand. IEEE Trans Smart Grid 2012;3(1):394–403.
[28] Galus MD, Waraich RA, Noembrini F, Steurs K, Georges G, Boulouchos K, et al. Integrating power systems, transport systems and vehicle technology for electric mobility impact assessment and efficient control. IEEE Trans Smart Grid 2012;3(2):934–49.
[29] Bessani M, Fanucchi RZ, Delbem ACC, Maciel CD. Impact of operators' performance in the reliability of cyber–physical power distribution systems. IET Gener Transm Distrib 2016;10(11):2640–6.
[30] Wu G, Wang G, Sun J, Chen J. Optimal partial feedback attacks in cyber–physical power systems. IEEE Trans Automat Contr 2020;65(9):3919–26.
[31] Jahromi AA, Kemmeugne A, Kundur D, Haddadi A. Cyber–physical attacks targeting communication-assisted protection schemes. IEEE Trans Power Syst 2020;35(1):440–50.
[32] Li Y, Wang Y, Hu S. Online generative adversary network based measurement recovery in false data injection attacks: a cyber–physical approach. IEEE Trans Industr Inform 2020;16(3):2031–43.
[33] Liu Y, Lu D, Deng L, Bai T, Hou K, Zeng Y. Risk assessment for the cascading failure of electric cyber–physical system considering multiple information factors. IET Cyber-Phys Syst Theory Appl 2017;2(4):155–60.
[34] Sun X, Liu Y, Deng L. Reliability assessment of cyber–physical distribution network based on the fault tree. Renew Energy 2020;155:1411–24.
[35] Xin S, Guo Q, Sun H, Zhang B, Wang J, Chen C. Cyber–physical modeling and cyber-contingency assessment of hierarchical control systems. IEEE Trans Smart Grid 2015;6(5):2375–85.
[36] Falahati B, Fu Y. Reliability assessment of smart grids considering indirect cyber–power interdependencies. IEEE Trans Smart Grid 2014;5(4):1677–85.
[37] Xu L, Guo Q, Yang T, Sun H. Robust routing optimization for smart grids considering cyber–physical interdependence. IEEE Trans Smart Grid 2019;10(5):5620–9.
[38] Adefarati T, Bansal RC. Reliability, economic and environmental analysis of a microgrid system in the presence of renewable energy resources. Appl Energy 2019;236:1089–114.
[39] Liu W, Gong Q, Han H, Wang Z, Wang L. Reliability modeling and evaluation of active cyber physical distribution system. IEEE Trans Power Syst 2018;33(6):7096–108.
[40] Cheng L, Chang Y, Lin J, Singh C. Power system reliability assessment with electric vehicle integration using battery exchange mode. IEEE Trans Sustain Energy 2013;4(4):1034–42.
[41] Wang X, Karki R. Exploiting PHEV to augment power system reliability. IEEE Trans Smart Grid 2017;8(5):2100–8.
[42] Li W. Study on urban rail transit intelligent and integrated dispatch manage system [dissertation]. Beijing: Beijing Jiaotong University; 2006. Chinese.
[43] Wan Y, Cao J, Zhang S, Tu G, Lu C, Xu X, et al. An integrated cyber–physical simulation environment for smart grid applications. Tsinghua Sci Technol 2014;19(2):133–43.
[44] Gao G. Critical technologies and implementation program of common information platform based on ATMS [dissertation]. Changchun: Jilin University; 2005. Chinese.
[45] Bowman JL, Ben-Akiva ME. Activity-based disaggregate travel demand model system with activity schedules. Transp Res Part A Policy Pract 2001;35(1):1–28.
[46] Nie Y, Wang X, Cheng KWE. Multi-area self-adaptive pricing control in smart city with EV user participation. IEEE Trans Intell Transp Syst 2018;19(7):2156–64.
[47] Santos A, McGuckin N, Nakamoto HY, Gray D, Liss S. Summary of travel trends: 2009 national household travel survey. Washington, DC: US Department of Transportation, Federal Highway Administration; 2011.
[48] Billinton R, Jonnavithula S. A test system for teaching overall power system reliability assessment. IEEE Trans Power Syst 1996;11(4):1670–6.
[49] Deng L, Liu Y, Yu Y, Bai T. Reliability assessment of distribution network CPS considering whole fault processing. Electr Power Autom Equip 2017;37(12):22–9. Chinese.
[50] Beijing Municipal Commission of Transport. Real-time traffic condition [Internet]. Beijing: Beijing Municipal Commission of Transport; 2019 [cited 2021 Apr 15]. Available from: http://jtw.beijing.gov.cn/.
[51] Weather Post website. Historical weather of Beijing [Internet]. Anhui: Weather Post website; 2019 [cited 2021 Apr 15]. Available from: http://www.tianqihoubao.com/lishi/beijing.html. Chinese.